Comparison of Infinite Element Models

Arkadiusz Zak, Magdalena Palacz, Marek Krawczuk, Łukasz Dolinski, Łukasz Skarbek

7th European Workshop on Structural Health Monitoring
July 8-11, 2014. La Cité, Nantes, France

COMPARISON OF INFINITE ELEMENT MODELS

Arkadiusz Żak[1], Magdalena Palacz[1], Marek Krawczuk[1], Łukasz Doliński[1], Łukasz Skarbek[1]

[1] *Gdańsk University of Technology, Faculty of Electrical and Control Engineering, ul. Narutowicza 11/12, 80-233 Gdańsk, Poland*

mpalacz@pg.gda.pl

ABSTRACT

The main objective of this paper is to show the comparison of two models of infinite absorbing layer with increasing damping in numerical investigations of elastic wave propagation in unbounded structures. This has been achieved by the Authors by a careful investigation of two different engineering structures characterised by gradually increasing geometrical and mathematical description complexities. The analysis included propagation of longitudinal elastic waves in a 1-D half-infinite isotropic rod, modelled according to the classical 1-mode theory of rods as well as propagation of coupled shear and flexural elastic waves in a 1-D half-infinite isotropic beam modelled according to the Timoshenko beam theory. The comparison of both models has been not only presented by the Authors, but also advantages and disadvantages of both of them have been discussed.

KEYWORDS : *wave propagation modelling, damage detection*

1. INTRODUCTION

Structural Health Monitoring (SHM) is referred as the process of implementing damage detection and the health characterisation strategy for engineering structures. The SHM process involves observation of a system over time using periodically sampled dynamic response measurements from an array of sensors, the extraction of damage-sensitive features from these measurements, and the statistical analysis of these features so as to determine the current state of system health [1].

For structural damage detection procedures very attractive parameters are propagating waves. Although their interaction with damage gives notable damage indications, but the complexity of their propagation pattern is the major difficulty for numerical modelling as well as for the system response interpretation [2]. Among many numerical modelling techniques offering models suitable for wave propagation the most popular are the spectral element method (SEM) proposed by Doyle [3] and the spectral finite element method (SFEM) proposed by Patera [4].

In the SFEM spectral series are applied for solutions of partial differential equations, while at the same time its basic ideas remain analogous to the classical finite element method (FEM). Its main assumption is the application of orthogonal Lobatto polynomials as approximation functions defined as based on the Gauss-Lobatto-Legendre (GLL) integration points. As a consequence of that the inertia matrix obtained can be diagonal (2-D problems) making the total cost of numerical calculations much less demanding. But primarily, thanks to the orthogonality of the approximation polynomials the SFEM method is characterised by exponential convergence [5].

2. NUMERICAL CONSIDERATIONS

The concept of an absorbing layer with increasing damping (ALID) is well described in [6], however it should be mentioned at this point that this idea dates back to 1980s [7]. This concept can be explained by considering a simple 1-D equation of motion in the time domain, written for the layer using the FEM convention [8], as:

$$[\mathbf{M}]\{\ddot{q}\} + [\mathbf{C}]\{\dot{q}\} + [\mathbf{K}]\{q\} = \{F\} \tag{1}$$

where $[\mathbf{M}]$, $[\mathbf{C}]$ and $[\mathbf{K}]$ are the characteristic inertia, damping and stiffness matrices, while $\{q\}$ and $\{F\}$ are the vectors of nodal displacements and forces dependent on the x co-ordinate only. The symbols $\dot{\square} = \frac{\partial}{\partial t}$ and $\ddot{\square} = \frac{\partial^2}{\partial t^2}$ denote the first and second time derivatives, respectively.

Under assumption that the damping matrix $[\mathbf{C}]$ within the ALID is a linear combination of both the inertia $[\mathbf{M}]$ and the stiffness $[\mathbf{K}]$ matrices, as well as that harmonic waves can propagate only along the x-axis, it can be written that:

$$[\mathbf{C}] = a(x)[\mathbf{M}] + b(x)[\mathbf{K}], \quad \{q\} = \{\hat{q}\}e^{-i\omega t}e^{ikx} \tag{2}$$

where ω and k are the angular frequency and the wave number, while $a(x)$ and $b(x)$ are certain smooth scaling functions that vary along the depth of the ALID in the following manner:

$$a(0) = b(0) = 0, \quad a(l) = b(l) = 1 \tag{3}$$

where $x = 0$ corresponds to the structure-layer interface and $x = l$ to the full length of the layer. The symbol $i = \sqrt{-1}$ denotes the imaginary unit, while $\{\hat{q}\}$ is the vector of nodal displacement amplitudes.

After substitution of relations (2) into (1) and necessary rearrangement of terms the original equation of motion in the time domain (1) can represented in the frequency domain as:

$$-\rho\left(1 + i\frac{a(x)}{\omega}\right)[\tilde{\mathbf{M}}]\omega^2\{q\} + E\left(1 - i\omega b(x)\right)[\tilde{\mathbf{K}}]\{q\} = \{F\} \tag{4}$$

with $[\mathbf{M}] = \rho[\tilde{\mathbf{M}}]$ and $[\mathbf{K}] = E[\tilde{\mathbf{K}}]$, and where ρ and E are the frequency independent material density and elastic modulus, respectively.

From the equation of motion (4) it arises that both density ρ and elastic modulus E can be considered as frequency dependant within the ALID:

$$\rho(\omega) = \rho\left(1 + i\frac{a(x)}{\omega}\right), \quad E(\omega) = E\left(1 - i\omega b(x)\right) \tag{5}$$

what allows to express the frequency dependant wave number $k(\omega)$ as:

$$k^2(\omega) = \omega^2\frac{\rho(\omega)}{E(\omega)} = \omega^2\frac{\rho}{E}(c + id) \tag{6}$$

where:

$$c = \frac{1 - a(x)b(x)}{1 + b^2(x)\omega^2}, \quad d = \frac{a(x) + b(x)\omega}{\omega + b^2(x)\omega^3} \tag{7}$$

Based on relations (7) it can be noted that the wave number $k(\omega)$ is complex with its real and imaginary part remaining positive in the case of elastic waves propagating within the ALID in the positive direction [6]. All such waves are attenuated and their wave numbers vary over the length of the layer.

It should be mentioned here that the part of the damping matrix $[\mathbf{C}]$ proportional to the stiffness matrix $b(x)[\mathbf{K}]$ strongly affects numerical solving of the equation of motion (1). In a general case of the TD-SFEM and problems related with propagation of elastic waves the explicit scheme of central differences is commonly used [5], as the scheme can take full advantage of the diagonal (1-D or 2-D problems) or semi-diagonal (3-D problems) forms of the characteristic inertia $[\mathbf{M}]$ and preferably damping $[\mathbf{C}]$ matrices. However, the part of the damping matrix $b(x)[\mathbf{K}]$ is consistent or full and cannot be effectively diagonalised in this case. Moreover, it also strongly affects the stability of the central difference scheme significantly increasing its minimal time step. On the other hand the part of the damping matrix $[\mathbf{C}]$ proportional to the inertia matrix, i.e. $a(x)[\mathbf{M}]$, is practically free of these drawbacks. For those reasons the damping matrix $[\mathbf{C}]$ is usually assumed in the form:

$$[\mathbf{C}] = a(x)[\mathbf{M}], \quad b(x) = 0 \tag{8}$$

It can be further assumed that the functions $a(x)$ can be expressed as:

$$a(x) = 10^{\alpha} x^{\beta}, \quad \alpha, \beta > 0 \tag{9}$$

which allows to express relation (6) is a simplified form:

$$k^2(\omega) = \omega^2 \frac{\rho}{E} \left(1 + i \frac{10^{\alpha} x^{\beta}}{\omega} \right) \tag{10}$$

In the remaining part of this paper the damping matrix $[\mathbf{C}]$ proportional only to the inertia matrix $[\mathbf{M}]$ is considered, which following relation (9) can be presented as:

$$[\mathbf{C}] = 10^{\alpha} x^{\beta} [\mathbf{M}], \quad x \in [0, l] \tag{11}$$

Appropriate selection of the values of α and β parameters, as well as the length l of the ALID, has a great influence on the layer damping properties. In the opinion of the Authors these values should stay as closely correlated with the characteristics of propagating elastic waves in order to serve as general guidelines in numerical calculations, as it is presented in the following sections of this paper.

3. CALCULATIONS

All results of numerical simulations presented in this paper were obtained by the use of the TD-SFEM [5]. The results were divided into two parts. In all cases considered hereafter appropriate spectral finite elements were employed, built based on the 5-th order Lobatto approximation polynomials [5]. In all these cases the associated equations of motion were solved by the explicit scheme of central differences with the diagonal inertia $[\mathbf{M}]$ and damping $[\mathbf{C}]$ characteristic matrices. Numerical calculations were carried out assuming isotropic material properties. For that purpose the following material properties of an aluminium alloy were used: elastic modulus $E = 72.5$ GPa, Poisson's ratio $\nu = 0.33$ and material density $\rho = 2900$ kg/m^3.

3.1 Semi-infinite isotropic rod

The geometry of a semi-infinite isotropic rod under investigation is presented in Fig. 1. The assumed length of the rod is $L = 1.5$ m, while the length of the ALID, representing the part of the rod extending to infinity, is denoted as l and is assumed as varying. The diameter of the rod is $d = 2r = 10$ mm. In case of SEM method the rod element was modelled with one element as the cross section was constant along the rod length. For the SFEM method the rod was modelled with 75 spectral finite elements defined according to the classical 1-mode theory of rods [9].

As an excitation force an 8-pulse sine signal modulated by the Hann window was used, acting at the origin of the co-ordinate system, as presented in Fig. 1. The amplitude of the excitation force acting along x-axis was 1 N, while its frequency was 200 kHz. The free type of boundary conditions was used. The total calculation time covered 500 μs and was divided into 2500 time steps.

It should be noted here that according to the applied classical 1-mode theory of rods [9] symmetric (longitudinal) elastic waves propagating within the rod are non-dispersive. Their phase and group velocities c_p and c_g are constant and equal to 5000 m/s in the current case. That fact greatly simplified the analysis that covered the influence of the α and β parameters on the damping capability of the ALID, noted as δ. This capability was expressed in terms of the ratio of energy E_1 to energy E_2 calculated for the same longitudinal displacement component signal $u_x(x,t)$ at two selected time instances t_1 and t_2 before entering and after leaving the layer:

$$\delta = 10 \log_{10} \frac{E_1}{E_2} \tag{12}$$

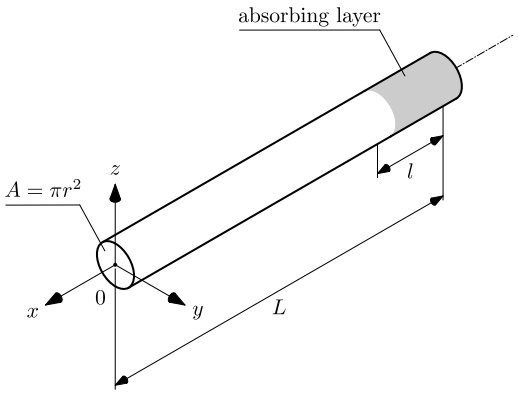

Figure 1 : Geometry of an isotropic rod/beam with an absorbing layer.

with:

$$E_1 = \sum_{i=1}^{N} |u_x(x_i,t_1)|^2, \quad E_2 = \sum_{i=1}^{N} |u_x(x_i,t_2)|^2 \tag{13}$$

where N is the total number of degrees of freedom of the rod numerical model. For calculations of the energies E_1 and E_2 the FFT of signals $u_x(x_i,t_1)$ and $u_x(x_i,t_2)$ were employed.

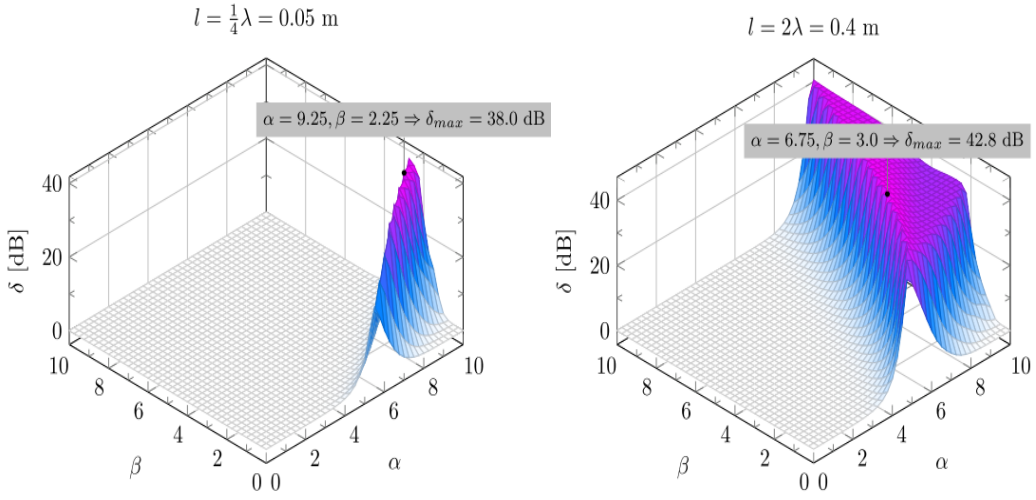

Figure 2 : Damping capability δ as a function of α and β parameters for an absorbing layer of 0.05m and 0.4 m.

In the case of the rod under consideration the time t_1 was selected as 40 μs. That enabled the complete formation of the excitation signal, which length λ was 0.2 m. The time t_2 was selected as 500 μs. The selected values of t_1 and t_2 correspond to wave propagation distances of 0.2 m and 2.5 m.

As the first the influence of the values of the α and β parameters was analysed on the damping capability of the layer δ. The length l of the ALID was an additional parameter of the analysis. Various values of the α and β parameters were tested within the range from 0 to 10 at 41 uniformly distributed discrete points. The exemplary results obtained are presented in Fig. 2.

It can be immediately noted that the values of the α and β parameters must be very carefully selected and closely correlated not only with the length of propagating elastic waves λ, but also with the length l of the ALID. It can be also seen that in a wide range of their values the ALID has practically no damping capability. This capability arises in a narrow band around certain values of the α and β

parameters. For obvious reasons an increase in the length l of the ALID extends the effective damping ability of the layer onto a wider range of the values of the α and β parameters.

The least effective damping was observed when the length l of the ALID was a quarter of the length of propagating elastic waves λ, as seen from left hand-side of Fig. 2. In this case the maximum value of the damping effectiveness δ reached 38.0 dB for the values of the α and β parameters 9.25 and 2.25, respectively. In comparison to that the most effective damping was achieved when the length l of the ALID was double the length of propagating elastic waves λ, as seen from right hand-side of Fig. 2. In this case the maximum value of the damping effectiveness δ reached 42.8 dB for the values of the α and β parameters 6.75 and 3.0, respectively.

It should be noted that an increase in the length l of the ALID resulted in a decrease in the values of the α and β parameters corresponding to the layer maximum damping capacity δ, as long as the length l of the ALID did not exceed the length of propagating elastic waves λ, as presented in Fig. 2. However, from a computational point of view the length l of the ALID should be selected as an optimal minimum. Therefore in the following cases discussed in this paper this length was always selected as equal to, or double, the length of propagating elastic waves λ.

As the second wave propagation patterns were investigated. They were calculated and obtained for the same rod at selected values of the α parameter. Following the results presented in Fig. 2 the value of the β parameter was kept constant and equal to 3, while the length of the absorbing layer l was assumed as double the length of propagating elastic waves λ. The damping capability δ was calculated based on the same formula (12). The results obtained are presented in Fig. 3.

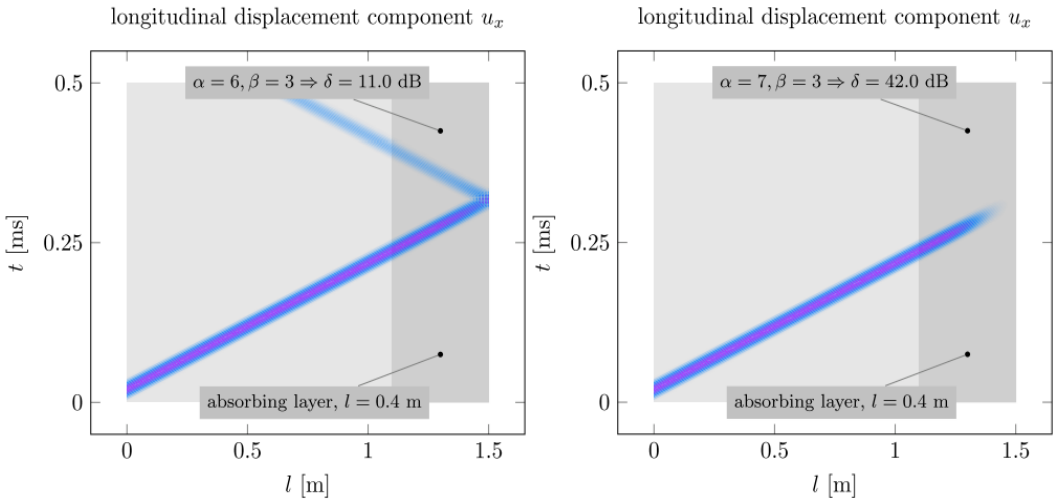

Figure 3 : Wave propagation patterns for the longitudinal displacement component u_x of longitudinal elastic waves propagating within an isotropic rod with an absorbing layer ($\alpha = 6, \beta = 3, l = 0.4$ m and $\alpha = 7, \beta = 3, l = 0.4$ m).

It can be seen that for the given length l of the ALID ($l = 2\lambda = 0.4$) the value of the α parameter has a strong influence of the wave propagation patterns. It should be noticed that a small variation in this parameter has a dramatic consequence on the performance of the layer. When the α parameter equal to 6 this effectiveness increases to 11.0 dB, while for the α parameter equal to 7 it reaches 42.0 dB as presented in Fig. 3.

Compared to the results obtained with ALID there are presented results calculated with SEM [3] for two cases - spectral rod element with a throw-off element working as a gap for leaking energy out of the system (Fig. 4). The drawing shown on the left hand-side in Fig. 4 is a result obtained with an assumption, that the throw-off has a value of 0.5. In this figure slight reflections may be noticed - its background is in the symmetric nature of the Inverse Fourier Transformation symmetry. The drawing

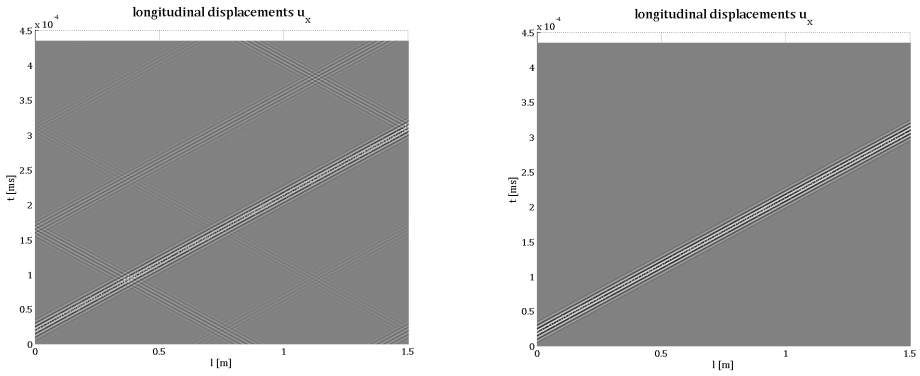

Figure 4 : Wave propagation patterns for the longitudinal elastic waves propagating within an isotropic rod - SEM model with a throw-off element on the right hand-side.

from right hand-side in the same Figure shows full throw-off element. As it can be easily noticed using SEM with its throw-off element is not quite precise while damping characteristics need to be analysed. For this purpose the Authors recommend considering more accurate numerical models, like developed combination of ALID and TD-SFEM methodology.

3.2 1-D semi-infinite isotropic beam

The analysis of propagation of bending elastic waves is much more complex. In order to perform this analysis the classical 1-mode theory of rods [9] was replaced by the 2-mode Timoshenko theory of beams [10]. In this theory two independent wave propagation modes can be observed that are characterised by different propagation velocities. These are the primary anti-symmetric (flexural) mode A_0 and the primary anti-symmetric shear mode SH_1 [5].

In the current case the geometry of a semi-infinite isotropic beam under investigation represents the same Fig. 1. However, the assumed length of the beam is $L = 2.0$ m. As before the length of the ALID, representing the part of the beam extending to infinity, and denoted as l, is assumed as varying. The diameter of the beam is also $d = 2r = 10$ mm. The beam was modelled by 100 spectral finite elements defined according to the 2-mode Timoshenko theory of beams [10]. The form and the amplitude of the excitation acting along z-axis were the same, while its frequency was selected as 100 kHz. The free type of boundary conditions was used. The total calculation time covered 1000 μs and was divided into 5000 time steps.

Because of the dispersive nature of the elastic waves propagating within the beam under investigation their phase and group velocities are different and frequency dependent. For the given excitation frequency of 100 kHz the group velocities of the primary flexural mode A_0 and the primary anti-symmetric shear mode SH_1 can be identified as 2750 m/s and 4900 m/s, both calculated based on the applied 2-mode Timoshenko theory of beams. As a consequence of different propagation velocities the two modes form two signals of different lengths λ_1 and λ_2 equal to 0.22 m and 0.39 m, respectively.

Results presented in Fig. 5 indicate that when the length l of the ALID is selected as equal to the longest waves propagating within the beam λ_2 the values of the α and β parameters have great influence on the the damping effectiveness. It can also be noticed from Fig. 5 that for the values of the α and β parameters equal to 5 and 3 the damping capability δ of the ALID can be negative in the case of the longitudinal displacement component u_x. This unusual physical behaviour is a direct consequence of the mode coupling and conversion.

It is well seen that as a result of the excitation both A_0 and SH_1 wave modes propagate together. Due to the coupling between the modes, which originates from shear deformation during wave motion, each boundary reflection of either A_0 and SH_1 mode results in simultaneous generation of both these

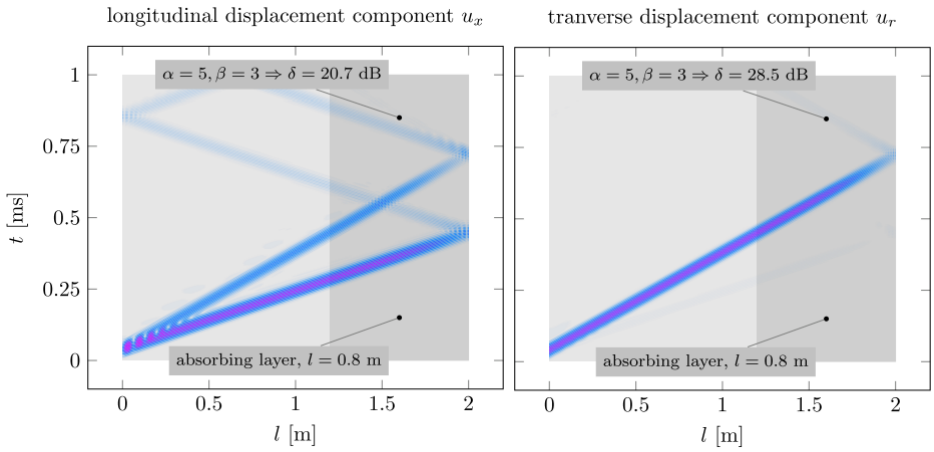

Figure 5 : Wave propagation patterns for the transverse displacement component u_x and u_r of flexural elastic waves propagating within an isotropic beam with an absorbing layer ($\alpha = 5, \beta = 3, l = 0.4$ m).

modes. During the reflection of the incident A_0 mode, the amplitude of the longitudinal component u_x of the generated SH_1 increases at the cost of the transverse component u_r of the same incident A_0 mode, as illustrated by Fig. 5.

It is interesting to note that the results presented in Fig. 5 correspond well to the results discussed previously and presented in Fig. 3. So, when the length l of the ALID is increased to double the length of the longest waves propagating within the beam λ_2 the overall damping effectiveness δ of the ALID is also increased, however, the values of the α and β parameters must be chosen appropriately in order to maximise the layer performance.

Considering the SEM model with its throw-off element for a beam it has to be mentioned, that the results have similar nature as in case of rod element. The analysis precision has not satisfactory level, that is the reason why the Authors recommend using AlID method.

CONCLUSIONS

Nowadays numerical simulations play a very important role in engineering sciences as a source of very valuable information about structural behaviour. Therefore it is very important to develop and test more efficient and more sophisticated models that enable their users a deeper insight into simulated phenomena. Problems related with propagation of elastic waves in semi-infinite or infinite structural elements remain not only very important, but also very demanding due to the complexity of simulated phenomena as well as the geometrical properties of investigated structures. The concept of an absorbing layer with increasing damping (ALID) appears as a very good solution, especially when combined with such an effective numerical tool as the spectral finite element method in the time domain (TD-SFEM).

The results presented in this work allow the Authors to formulate certain conclusions about the application and effectiveness of the ALID in the case of wave propagation related problems. The following conclusions can be drawn:

- It has been shown by the Authors that the concept of the ALID can be effectively combined with the TD-SFEM.
- It has been demonstrated numerically by use of the TD-SFEM that the ALID can be applied in order to mimic semi-infinite boundary conditions in the case of wave propagation problems in 1-D rod and beam.
- It has been shown that SEM may give improper results due to its mathematical limitations.

- The properties of the ALID should always be closely correlated with the characteristics of propagating elastic waves.
- The length of the ALID should be selected as close to the length or double the length of the longest waves propagating in the structure.
- It is suggested by the Authors that for the ALID lengths equal to the longest length of propagating elastic waves the values of the α and β parameters are selected as equal to 6 and 1, respectively.
- However, it is recommended by the Authors to use layers of the lengths equal to double the longest length of propagating elastic waves. In this case the values of the α and β parameters are selected as equal to 7 and 3, respectively.

4. ACKNOWLEDGEMENTS

The Authors of this work would like to gratefully acknowledge the support for their research provided by the Academic Computer Centre in Gdańsk. All results presented in this paper have been obtained by the use of the software available at the Academic Computer Centre in Gdańsk.

The Authors would also like to to gratefully acknowledge the financial support for their research provided by National Science Centre based on the decision number DEC-2012/07/B/ST8/03741.

REFERENCES

[1] B. Dawson. Vibrational condition monitoring techniques for rotating machinery. *Shock Vibration Digest*, 8(12):3, 1976.

[2] B. C. Lee and W.J. Staszewski. Lamb wave modelling for damage detection ii. damage monitoring strategy. *Smart Materials and Structures*, 16:260–274, 2007.

[3] J. F. Doyle. *Wave Propagation in Structures. Spectral Analysis Using Fast Discrete Fourier Transforms*. Springer-Verlag, New York, 1997.

[4] A. T. Patera. A spectral element method for fluid dynamics: Laminar flow in a channel expansion. *Journal of Computational Physics*, 54:468–488, 1984.

[5] W. Ostachowicz, P. Kudela, M. Krawczuk, and A. Żak. *Guided Waves in Structures for SHM*. Wiley & Sons, West Sussex, 2012.

[6] M. B. Drozdz. *Efficient finite element modelling of ultrasound waves in elastic media. Ph.D. Thesis*. Imperial College of Science Technology and Medicine. University of London, London, 2008.

[7] M. Israeli and S. A. Orszag. Approximation of radiation boundary conditions. *Journal of Computational Physics*, 41:115–135, 1981.

[8] O. C. Zienkiewicz. *The Finite Element Method*. McGraw-Hill Book Company, London, 1989.

[9] A. Żak and M. Krawczuk. Assessment of rod behaviour theories used in spectral finite element modelling. *Journal of Sound and Vibration*, 329:2099–2113, 2010.

[10] A. Żak and M. Krawczuk. Assessment of flexural beam behaviour theories used for dynamics and wave propagation problems. *Journal of Sound and Vibration*, 331:5715–5731, 2012.